JOC The Journal of Organic Chemistry

Article

pubs.acs.org/joc

Deep-Red Emissive BODIPY−Chlorin Arrays Excitable with Green and Red Wavelengths

Adam Meares,[†] Andrius Satraitis,[†] Nithya Santhanam, Zhanqian Yu, and Marcin Ptaszek*

Department of Chemistry and Biochemistry, University of Maryland, Baltimore County, 1000 Hilltop Circle, Baltimore, Maryland 21250, United States

Supporting Information

ABSTRACT: We report here the synthesis and characterization of BODIPY−chlorin arrays containing a chlorin subunit, with tunable deep-red (641−685 nm) emission, and one or two BODIPY moieties, absorbing at 504 nm. Two types of arrays were examined: one where BODIPY moieties are attached through a phenylacetylene linker at the 13- or 3,13-positions of chlorin, and a second type where BODIPY is attached at the 10-position of chlorin through an amide linker. Each of the examined arrays exhibits an efficient (≥0.80) energy transfer from BODIPY to the chlorin moiety in both toluene and DMF and exhibits intense fluorescence of chlorin upon excitation of BODIPY at ∼500 nm. Therefore, the effective Stokes shift in such arrays is in the range of 140−180 nm. Dyads with BODIPY attached at the 10-position of chlorin exhibit a bright fluorescence in a range of solvents with different polarities (i.e., toluene, MeOH, DMF, and DMSO). In contrast to this, some of the arrays in which BODIPY is attached at the 3- or at both 3,13-positons of chlorin exhibit significant reduction of fluorescence in polar solvents. Overall, dyads where BODIPY is attached at the 10-position of chlorin exhibit ∼5-fold brighter fluorescence than corresponding chlorin monomers, upon excitation at 500 nm.

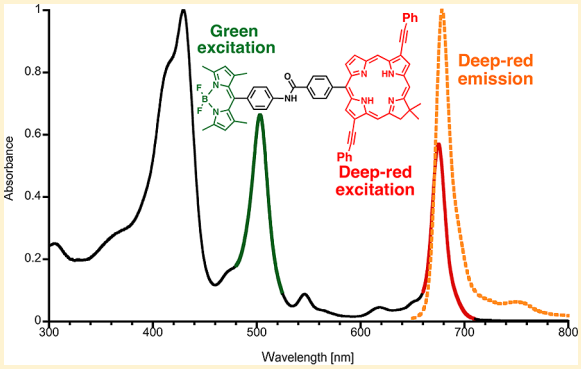

INTRODUCTION

Hydroporphyrins (chlorins and bacteriochlorins) are tetrapyrrolic macrocycles, which offer unique benefits for *in vivo* fluorescence imaging. They possess multiple absorption bands, e.g., the deep-red or near-IR Q_y band (650−700 nm for chlorins, 700−800 nm for bacteriochlorins), the Q_x band, which is located in the green range (500−520 nm), and *B* bands, which are located in the violet or UV spectral windows (400−430 nm for chlorins, 360−380 nm for bacteriochlorins).[1−4] Excitation at each of these absorption bands results in an emission in the deep-red (chlorin, 630−700 nm) or the near-IR (bacteriochlorin, 720−800 nm) spectral windows. Another beneficial feature of hydroporphyrins is their narrow (with full-width at half-width-at-half-of-maximum ∼12−20 nm) emission bands. Additionally, wavelengths of absorption and emission maxima for hydroporphyrins can be precisely tuned by substitution on the periphery of the macrocycles.[2−5] Both the latter properties should greatly facilitate applications of hydroporphyrins as fluorophores for multicolor imaging. Recently, our collaborative efforts have demonstrated that unique properties of hydroporphyrins are highly beneficial for construction of fluorescent probes for anticancer fluorescence-guided surgery.[6,7] It has been shown that, upon excitation with the green light (∼510 nm), a probe containing bacteriochlorin as a fluorophore results in near-IR emission (760 nm) with a large pseudo-Stokes shift (250 nm) and produces a very sharp near-IR image of target tumors located on the tissue surface, with a high tumor-to-background ratio.[6] This is apparently due to the large Stokes shift, which enables detection of a near-IR emission far from the excitation beam. As a result, both background fluorescence and detection of scattered light from the excitation source are diminished. Due to very shallow tissue penetration, green light is unable to excite fluorophores localized deeper in the tissue; these can only be detected and visualized upon excitation with the near-IR wavelengths. However, near-IR excitation, due to the small Stokes shift (∼10 nm) and tissue autofluorescence, produces blurred images with a tumor-to-background ratio lower than that observed for green excitation. Nevertheless, near-IR excitation can instead be used for detection of tumors localized below the tissue surface (or hidden behind mesentery or intestines), while green excitation can be used for precise determination of tumor margins. This "double-excitation" approach is not possible with fluorophores typically used for near-IR imaging (such as cyanines), since the latter do not possess an appreciable absorbance in the green spectral window.[6] Typical organic near-IR fluorophores usually exhibit a single, relatively narrow absorption band in the near-IR spectral window, due to their $S_0−S_1$ absorption, and their band corresponding to $S_0−S_2$ absorption is located in the UV spectral window (with $\lambda < 400$ nm).[8]

Subsequently, it has also been demonstrated that hydroporphyrins can be used for simultaneous visualization of two different cancer cells *in vivo* due to their narrow and tunable

Received: January 16, 2015
Published: March 24, 2015

DOI: 10.1021/acs.joc.5b00119
J. Org. Chem. 2015, 80, 3858−3869

emission bands.[7] Chlorins and bacteriochlorins have also been utilized by other groups for intracellular and *in vivo* fluorescence or photoaccoustic imaging.[9,10]

One of the limitations, which potentially might hamper the full exploitation of hydroporphyrins' properties in fluorescence-guided surgery, is the relatively low extinction coefficient for the Q_x band (~500 nm), which is in the range of ~8000−13 000 $M^{-1}\cdot cm^{-1}$ for chlorins,[11] and 35 000−39 000 $M^{-1}\cdot cm^{-1}$ for bacteriochlorins.[12] These values are substantially lower in comparison to typical fluorophores used in fluorescence imaging (>100 000 $M^{-1}\cdot cm^{-1}$) and results in substantially lower fluorescence brightness upon visible excitation (for a compilation of the brightness of typical near-IR fluorophores see ref 13).

We propose to increase the fluorescence brightness of hydroporphyrins, upon excitation at ~500 nm, by utilizing an auxiliary chromophore, strongly absorbing in the green region, and capable of transferring excitation energy to hydroporphyrins. Hydroporphyrins in energy transfer arrays might function as both energy donors and acceptors, which was utilized in the construction of arrays with potential biomedical or energy-related applications.[9,14−22] A dyad containing green light-absorbing rhodamine as an energy donor and a chlorophyll *a* derivative as an energy acceptor has been reported, and an efficient energy transfer from rhodamine to chlorin moiety has been determined.[9] We anticipated that positively charged rhodamine might be an efficient electron acceptor for a photoexcited chlorin, and thus might significantly quench the chlorin fluorescence in resulting arrays constructs (as it was reported for analogous porphyrin−rhodamine arrays).[23,24] Therefore, as an auxiliary chromophore, we have chosen a boron complex of dipyrrin (often referred to as BODIPY).[25−28] BODIPY is a class of neutral molecules, broadly utilized as fluorescent labels and probes, with molar excitation coefficients up to 100 000 $M^{-1}\cdot cm^{-1}$, and usually possessing high fluorescence quantum yields. There are numerous examples of energy transfer dyads where BODIPY derivatives have been employed as energy donor,[25,26] including these with red or near-IR emitting acceptors,[27] and a wide range of BODIPY−porphyrin dyads.[28] To the best of our knowledge, the only examples of BODIPY−hydroporphyrin arrays are the aza-BODIPY−chlorin dyads reported by Tamiaki, where a chlorophyll-type moiety functions as an energy donor, and aza-BODIPY as an energy acceptor.[22]

In this paper, we describe the synthesis and evaluation of optical properties of BODIPY−chlorin arrays. Our goal was to establish a molecular architecture for arrays which assures bright emission of the chlorin acceptor upon excitation of the BODIPY donor, regardless of polarity of environment. This requires efficient energy transfer, and a lack of competitive processes, which might quench fluorescence of chlorin. The latter processes can be potentially devastating for the emission properties of dyads, as significant quenching of fluorescence of both donor and acceptor has been reported (for example, in BODIPY−phthalocyanine dyads[29]). One such process could be photoinduced electron transfer (PET), from photoexcited chlorin to BODIPY. Chlorins are known as a potent electron donor in their excited state,[18,30] and quenching of BODIPY fluorescence by PET is a well-known phenomenon.[31] Indeed, significant quenching of fluorescence in aza-BODIPY−chlorin dyads in polar solvents due to PET has been reported.[22]

Additionally, we have been searching for the BODIPY−chlorin dyad architecture which would provide versatility in tuning the absorption/emission wavelengths of chlorin. The wavelength of absorption and emission can be tuned by a substitution of chlorins at the 3- and 13-positions;[3,4] therefore, our construct should allow placing different substituents at these positions.

Toward these goals, we designed two types of arrays (Chart 1). In the first type [arrays **1-BDP**, **2-(BDP)$_2$**, and **Zn2-(BDP)$_2$**], a BODIPY unit is attached at the 13- and 3,13-positions, through a phenylethynyl linker. In these constructs, the linker functions also as an auxochrome which tunes emission properties of chlorin. In the second type (dyads **3-BDP**, **4-BDP**, and **Zn4-BDP**), a BODIPY unit is attached to a phenyl group localized at the 10-position of chlorin through an amide bond, while auxochromes (phenylethynyl groups) are placed independently at the 3- and 13-positions. Two corresponding Zn(II) chelates of some arrays were prepared [i.e., **Zn2-(BDP)$_2$** and **Zn4-BDP**] to evaluate the influence of metal complexation of chlorin on optical properties of resulting arrays. This selection of arrays enables us to examine properties of architectures for which the chlorin acceptor possesses a broad range of optical and redox properties, since both substitution at the 3,13-positions and zinc metalation markedly alter absorption/emission maxima, and redox properties of chlorins.[3,4,18] As benchmark donors, we investigated corresponding BODIPY derivatives, **BDP-TMS** and **BDP-NHBz**, and as benchmark acceptors, chlorin derivatives, **1**−**3** and **Zn2** (Chart 1).

RESULTS AND DISCUSSION

Synthesis. Syntheses of target BODIPY−chlorin arrays required two different strategies. The key reaction for the synthesis of **1-BDP** and **2-(BDP)$_2$** is Sonogashira coupling of bromosubstituted chlorins with a BODIPY derivative with a 4-ethynylphenyl substituent at the *meso* position (**BDP-H**). For the synthesis of **3-BDP** and **4-BDP**, we employed amide bond formation between chlorin derivatives possessing a carboxylic acid function and amine-functionalized BODIPY (**BDP-NH$_2$**). Both strategies utilize similar chlorin building blocks: chlorins **1-Br**, **2-Br$_2$**, and **3**, each possessing a 4-(methoxycarbonyl)-phenyl substituent at the 10-position. The synthesis of 13-bromochlorin **1-Br** has been previously reported.[20] Chlorins **2-Br$_2$** and **3** were synthesized using reported procedures for analogous derivatives (Scheme 1).[32,33] Thus, bromination of known formyldipyrromethane **5**[20] with 1 or 2 equivs of NBS provides 1-bromo-9-formyldipyrromethane **6-Br** (94% yield) or 1,2-dibromo-9-formyldipyrromethane **6-Br$_2$** (67% yield), respectively. Subsequent condensation of **6-Br** with tetrahydrodipyrrin **7**, and **6-Br$_2$** with 8-bromotetrahydrodipyrrin **7-Br**, followed by zinc-mediated oxidative cyclization, and demetalation provides **3** (25% yield), and **2-Br$_2$** (17% yield).

The synthesis of requisite **BDP-H** and **BDP-TMS** have been reported numerous times,[34] but here, we prepared it in a slightly different manner. We synthesized **BDP-H** following the established procedure for *meso*-substituted BODIPY, in one-pot, three-step reaction of 2,4-dimethylpyrrole with 4-[(trimethylsilyl)ethynyl]>benzaldehyde, catalyzed by a trace amount of TFA, followed by oxidation of the resulting dipyrromethane with DDQ, and complexation of the resulting dipyrrin by $BF_3\cdot OEt_2$ in the presence of Et_3N (Scheme 2), to afford **BDP-TMS** in 23% yield. The resulting **BDP-TMS** with a TMS-protected ethynyl functionality was deprotected using a previously reported procedure[34] (K_2CO_3 in MeOH/THF), to afford a target **BDP-H** in 60% yield.

Two different sets of copper-free Sonogashira cross-coupling conditions, reported previously for hydroporphyrins, were examined for reaction of **BDP-H** with chlorins **1-Br** and **2-Br$_2$**: $Pd_2(dba)_3$ in

DOI: 10.1021/acs.joc.5b00119
J. Org. Chem. 2015, 80, 3858−3869

Chart 1. Structures of BODIPY−Chlorin Arrays and Benchmark Monomers Discussed in This Paper

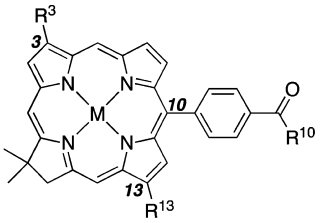

Compound	R^3	R^{13}	R^{10}	M
1-BDP	-H	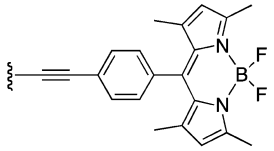	-OMe	H,H
2-(BDP)$_2$	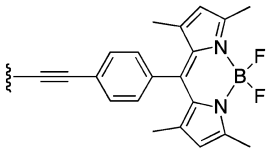	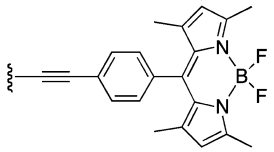	-OMe	H,H
Zn2-(BDP)$_2$	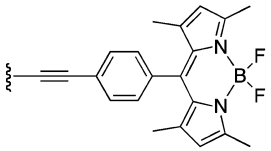	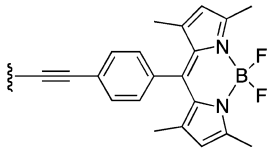	-OMe	Zn
3-BDP	-H	-H	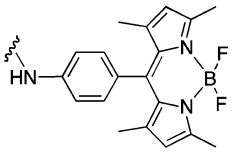	H,H
4-BDP	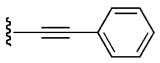	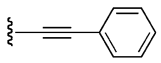	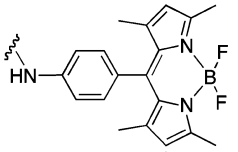	H,H
Zn4-BDP	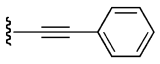	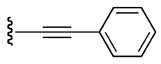	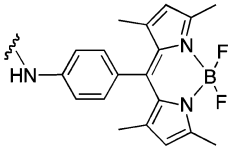	Zn
1	-H	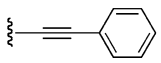	-OMe	H,H
2	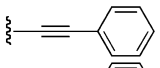	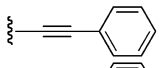	-OMe	H,H
Zn2	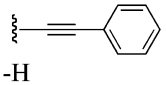	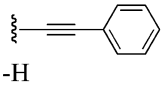	-OMe	Zn
3	-H	-H	-OMe	H,H

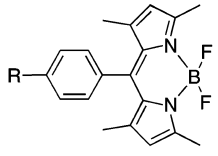

BDP-TMS R = 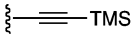

BDP-NHBz R = 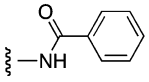

the presence of (*o*-tol)$_3$P in toluene/Et$_3$N,[33] and (PPh$_3$)$_2$PdCl$_2$ in DMF/Et$_3$N.[35] We found that the latter conditions provided desired products with better yields (52% and 47% for **1-BDP** and **2-(BDP)$_2$**, respectively, Scheme 3), and the target arrays were easier to purify. It is worth noting that reaction of analogous BODIPY, without methyl groups at pyrrole units, led

DOI: 10.1021/acs.joc.5b00119
J. Org. Chem. 2015, 80, 3858−3869

Scheme 1

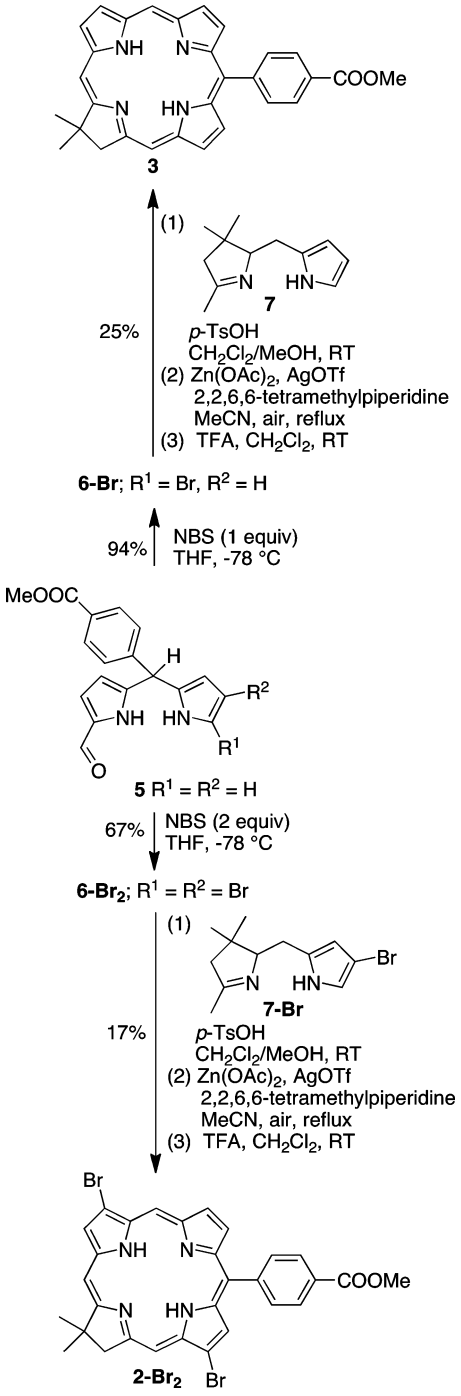

Scheme 2

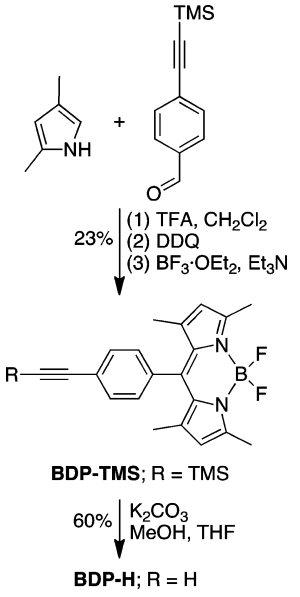

Scheme 3

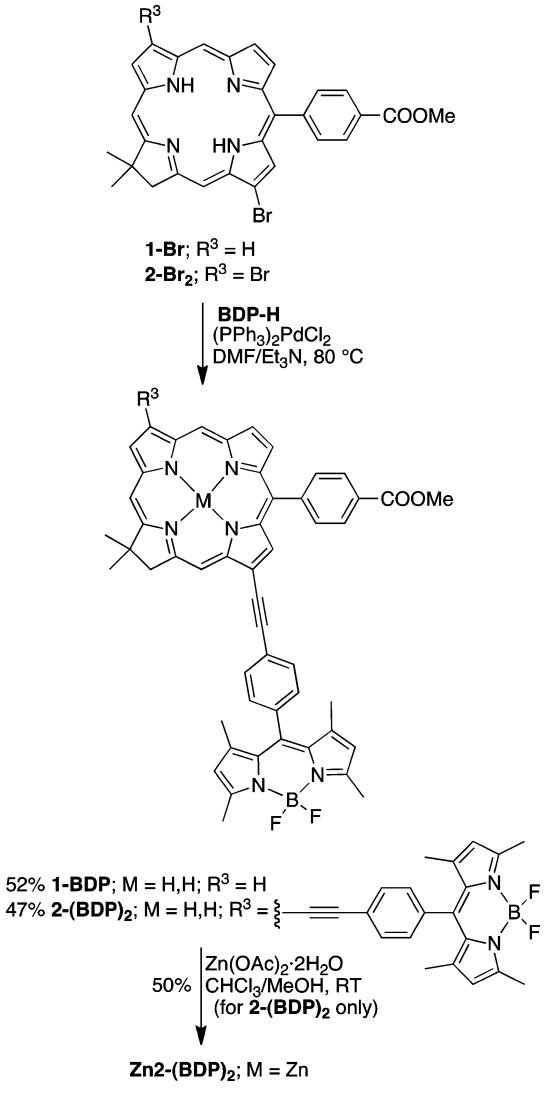

to decomposition of starting BODIPY, and no dyad was isolated.

Benchmark monomers **1** and **2** were obtained in analogous reactions of **1-Br** and **2-Br$_2$** with phenylacetylene in 84% and 60% yield, respectively (Scheme 4).

Dyads **3-BDP** and **4-BDP** were synthesized through the EDC-mediated coupling of known, amine-functionalized **BDP-NH$_2$**[36] with carboxylic acid functionalized chlorins (Scheme 5). Ester functions in **2** and **3** were quantitatively hydrolyzed to obtain respective chlorins, equipped with a free carboxylic acid moiety (**2-COOH** and **3-COOH**, structures not shown). The crude chlorin acids were reacted with **BDP-NH$_2$** in the presence of EDC hydrochloride and DMAP in DMF, to provide

DOI: 10.1021/acs.joc.5b00119
J. Org. Chem. 2015, 80, 3858−3869

Scheme 4

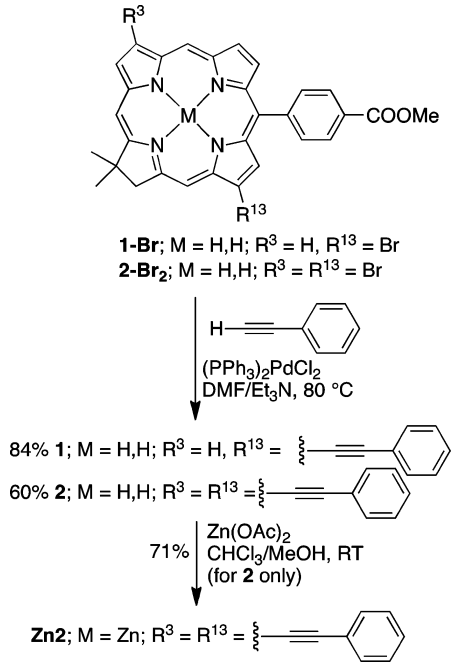

Scheme 5

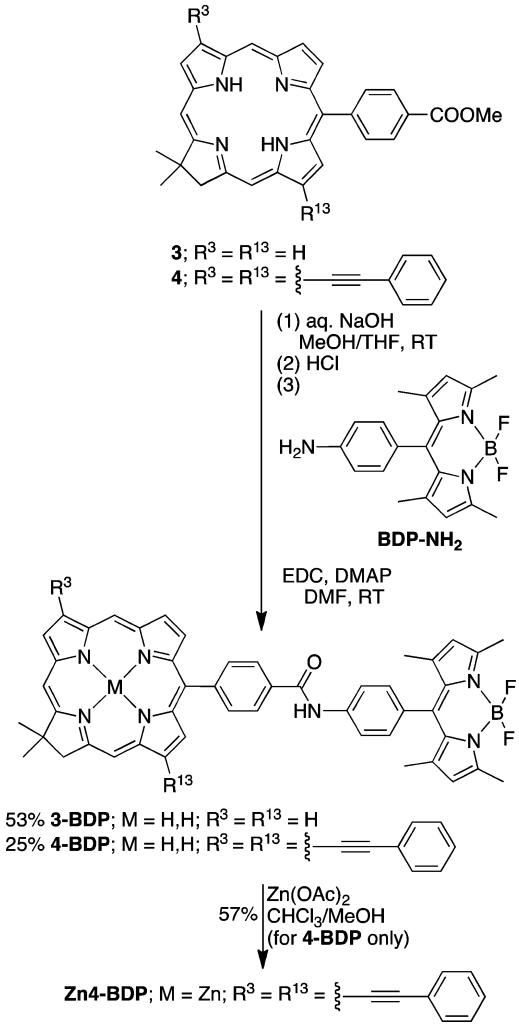

3-BDP and 4-BDP in 53% and 25% yield, respectively. Zn(II) chelates (Zn2-(BDP)$_2$, Zn4-BDP, and Zn2) were obtained in reaction of corresponding free bases with $Zn(OAc)_2$ in a $CHCl_3$/MeOH (5:1) mixture, in 50, 57, and 71% yield, respectively.

Benchmark monomer BDP-NHBz was obtained by reaction of BDP-NH$_2$ with benzoic acid, under analogous conditions as for 3-BDP and 4-BDP, to provide the desired product in 80% yield (Scheme 6).

Characterization. Target arrays were characterized by ^{1}H, ^{13}C, and ^{19}F NMR, LD-MS, and high-resolution MS. Triad 2-(BDP)$_2$ shows a low solubility in common organic solvents, which prevents recording of a good quality ^{13}C NMR and ^{19}F NMR spectra. The NMR spectra for all arrays are consistent with expected structures. In particular, ^{1}H NMR spectra for dyads 1-BDP, 3-BDP, and 4-BDP show resonances of protons from both the chlorin macrocycle and the BODIPY unit, with integration indicating a 1-to-1 ratio of chlorin to BODIPY. The ^{1}H NMR spectrum of 2-(BDP)$_2$ shows resonances from two, slightly nonequivalent BODIPY units.

Zinc complexation of 2 and 2-(BDP)$_2$ causes an extensive aggregation of the resulting Zn2 and Zn2-(BDP)$_2$, which results in a low solubility of both complexes in common solvents and makes the NMR characterization of these chelates problematic. We were able to obtain the ^{1}H NMR spectrum only for a crude sample of Zn2-(BDP)$_2$. After chromatographic purification and washing with MeOH and hexanes, the sample became insoluble, and no ^{1}H NMR spectra could be recorded. Nevertheless, the ^{1}H NMR spectrum of crude Zn2-(BDP)$_2$ showed a single chlorin, with chlorin and BODIPY resonances as expected, and HRMS shows m/z consistent with expected structures.

Absorption and Emission Properties. Absorption and emission properties of BODIPY−chlorin arrays as well as benchmark monomers are listed in Table 1, and spectra of arrays are presented in Figures 1 and 2 (absorption and emission spectra of monomers are presented in Figures S1 and S2, Supporting Information). Absorption spectra for chlorin derivatives

Scheme 6

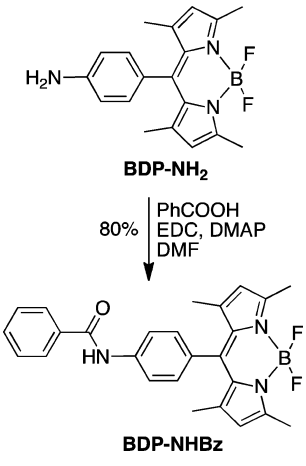

are consistent with these reported in the literature for analogous chlorins.[4,16] Chlorin monomers 1−3 and Zn2 exhibit strong B bands in the range of 403−430 nm, Q_x bands in the range of 499−514 nm, and Q_y bands progressively shifted with the number of conjugated substituents at 3,13-positions: 636 nm (3), 656 nm (1), and 675 nm (2). For Zn2, the absorption maximum of the Q_y band is shifted hypsochromically by 24 nm, compared to the corresponding free base.

DOI: 10.1021/acs.joc.5b00119
J. Org. Chem. 2015, 80, 3858−3869

Table 1. Absorption and Emission Properties of BODIPY−Chlorin Arrays and Benchmark Monomers[a]

compound	*B* [nm]	BODIPY/Q_x [nm]	Q_y [nm]	λ_{em} [nm]	Φ_f (toluene)[b]	Φ_f (DMF)[b]	ETE (toluene)[c]	ETE (DMF)[c]
1-BDP	404, 418	504	657	661	0.35	0.25	0.97	0.96
2-(BDP)$_2$	431	504, 548	678	683	0.41	0.38	0.96	0.97
3-BDP	406	503	636	641	0.21	0.20	0.90	0.92
4-BDP	428	503, 546	675	681	0.37	0.36	0.92	0.88
Zn2-(BDP)$_2$	427	504	658	661	0.37	0.011	0.88	[c]
Zn4-BDP	426	503	651	655	0.31	0.32	0.87	0.80
1	402, 417	506	656	659	0.33	0.34		
2	431	514, 546	675	681	0.37	0.36		
3	405	499	636	641	0.21	0.20		
Zn2	425	519	651	656	0.33	0.38		
BDP-TMS		504		517				
BDP-NHBz		503		516				

[a]Fluorescence quantum yields of the chlorin component upon excitation at the maximum of the *B* band. Φ_f was determined in air-equilibrated solvents, using tetraphenylporphyrin (TPP) in nondegassed toluene, as a standard (Φ_f = 0.070).[2] The estimated error in Φ_f is ±5%. [b]Efficiency of energy transfer, defined as a fluorescence quantum yield of the chlorin component upon excitation at the maximum of BODIPY absorbance over fluorescence quantum yield of chlorin component upon direct excitation at the maximum of the *B* band. [c]ETE could not be determined accurately due to a low intensity of fluorescence in DMF.

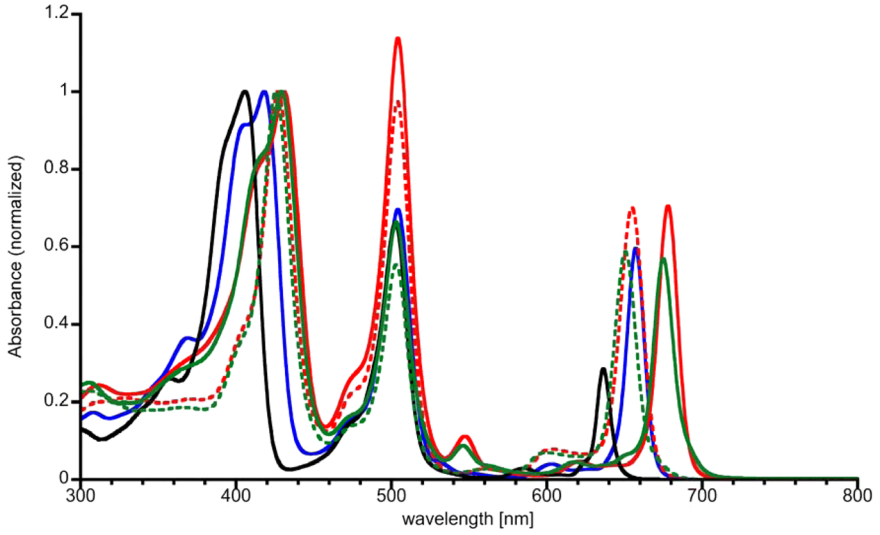

Figure 1. Absorption spectra of BODIPY−chlorin arrays: **1-BDP** (blue), **2-(BDP)$_2$** (red), **Zn2-(BDP)$_2$** (red, dashed), **3-BDP** (black), **4-BDP** (green), and **Zn4-BDP** (green, dashed). All spectra were taken in toluene at room temperature and normalized at the maximum of the *B* band of chlorin.

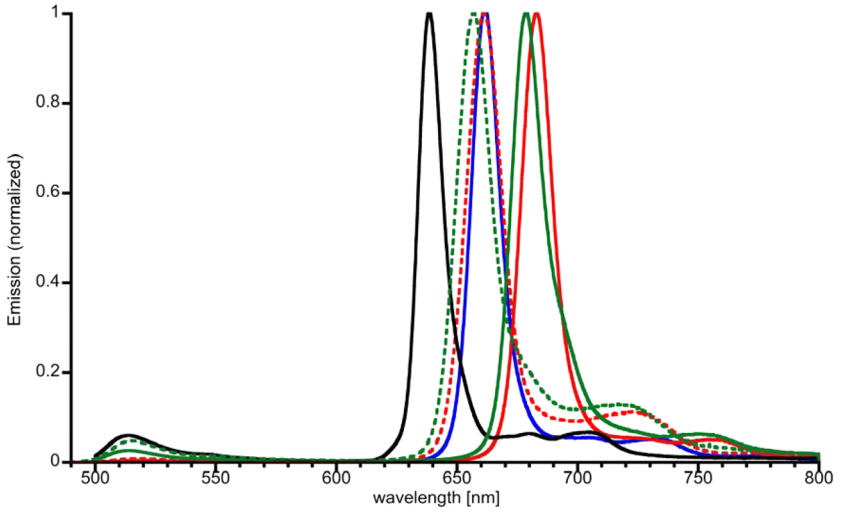

Figure 2. Normalized emission spectra of BODIPY−chlorin arrays: **1-BDP** (blue), **2-(BDP)$_2$** (red), **Zn2-(BDP)$_2$** (red, dashed), **3-BDP** (black), **4-BDP** (green), and **Zn4-BDP** (green, dashed). All spectra were taken in toluene at room temperature, with excitation at 475 nm.

DOI: 10.1021/acs.joc.5b00119
J. Org. Chem. 2015, 80, 3858−3869

Absorption spectra for arrays are essentially the sum of absorption spectra of their components (Figure 1, Table 1). For dyads **3-BDP**, **4-BDP**, and **Zn4-BDP**, the absorption maxima are identical to those for corresponding benchmark monomers **3**, **2**, and **Zn2**, respectively, while, for **1-BDP**, **2-(BDP)$_2$**, and **Zn2-(BDP)$_2$**, absorption bands for chlorin components are slightly shifted bathochromically by 1−7 nm compared to those for monomers **1**, **2**, and **Zn2**, respectively.

Emission spectra of chlorin benchmarks contain a narrow band, with relatively small Stokes shifts (1−6 nm). **BDP-TMS** and **BDP-NHBz** show a strong emission band at 517 and 516 nm, respectively. Emission spectra of all BODIPY−chlorin arrays are dominated by emission of the chlorin component. The maxima of chlorin emission in dyads **1-BDP**, **2-(BDP)$_2$**, and **Zn2-(BDP)$_2$** are shifted bathochromically by 2−5 nm, compared to those for benchmark monomers, while emission maxima for **3-BDP**, **4-BDP**, and **Zn4-BDP** appear exactly at the same wavelengths as for corresponding monomers. For each array, significant quenching of BODIPY fluorescence and almost exclusive emission from chlorin components are observed, even when BODIPY is directly excited at the wavelength where chlorins show a negligible absorbance (Figure 2). Excitation spectra, monitored at the wavelengths where chlorin components emit exclusively (not shown) closely resemble the corresponding absorption spectra. These indicate an efficient excitation energy transfer from BODIPY to the chlorin chromophore.

In order to quantitatively assess the energy transfer efficiency and presence of putative quenching processes in dyads, we determined the quantum yields of fluorescence of chlorin components for dyads and benchmark monomers in toluene and DMF (Table 1). We determined the relevant quantum yields in polar solvent to evaluate the possible quenching of chlorin fluorescence via PET, which is facilitated in polar solvents.

The fluorescence quantum yields in toluene for chlorin monomers increases with the number of conjugated substituents at the 3,13-positions: 0.21 for **3** (no substituents), 0.33 for **1** (one substituent), and 0.37 for **2** (two substituents). Quantum yield of emission for **Zn2** in toluene is 0.33. These data are consistent with those reported for analogous chlorin derivatives.[3,16] Quantum yields of fluorescence for monomers only slightly depend on solvent polarity, and values are nearly identical in DMF as in toluene (Table 1). Only for **Zn2**, we observed an increase in DMF (1.12-fold vs toluene). This increase we attributed to coordination of DMF to zinc, since such coordination has been reported to increase the fluorescence quantum yields for porphyrins.[37]

Quantum yields of fluorescence of chlorin components in dyads were determined by direct excitation of a given chlorin at the maxima of the *B* bands (410−430 nm), where the BODIPY component has a negligible absorbance. In nonpolar solvent (toluene), quantum yields for dyads are comparable (**3-BDP** and **4-BDP**), or even slightly higher (**1-BDP** and **2-BDP**) than those for the corresponding benchmark monomers (Table 1). This indicates that, in nonpolar solvents, the presence of a BODIPY unit does not quench the emission from chlorin.

In highly polar DMF, fluorescence of **1-BDP** is 0.71-fold of that in toluene, while, for **2-BDP**, it is 0.93-fold. Fluorescence quantum yields for **3-BDP** and **4-BDP** in DMF are nearly the same as those in toluene.

Fluorescence quantum yield for zinc complex **Zn2-(BDP)$_2$** in toluene (Φ_f = 0.37) is markedly higher than that for the corresponding chlorin benchmark **Zn2** (Φ_f = 0.33). However, fluorescence is reduced ∼30 times (Φ_f = 0.011) in DMF. On the contrary, fluorescence quantum yields for **Zn4-BDP** in both toluene and DMF are nearly identical.

The efficiency of energy transfer (ETE)[38] for BODIPY−chlorin arrays has been determined by comparison of fluorescence quantum yields of the chlorin acceptor upon excitation at the donor absorption maxima (504 nm, where chlorin absorbs much less than BODIPY), with fluorescence quantum yield obtained upon direct chlorin excitation at the maximum of the *B* band (Table 1). The ETE is relatively high (>0.90) in toluene and is rather independent of solvent polarity for **1-BDP** and **2-(BDP)$_2$**. For amide-linked **3-BDP** and **4-BDP**, ETE in DMF is slightly lower than that in toluene; however, it still exceeds 0.85. ETE for **Zn4-BDP** (0.87 and 0.80 in toluene and DMF, respectively) is noticeably lower than that for the corresponding free base; this also appears to be true for **Zn2-(BDP)$_2$** (0.87 in toluene; ETE for **Zn2-BDP** in DMF cannot be determined accurately, due to the low fluorescence intensity for excitations at both BODIPY and *B* bands maxima).

The efficient energy transfer between BODIPY and chlorin is likely driven by the overlap of the BODIPY emission band with the Q_x band of chlorin. The lower ETE for dyads containing chlorin zinc complexes can be explained by the lower oscillator strength of the Q_x band for zinc chlorin complexes, compared with free bases,[4,11] which results in lower spectral overlap. Despite the high and comparable ETE, both classes of arrays reported here exhibit a different behavior in polar solvent. The fluorescence quantum yields for amide-linked dyads are nearly the same in toluene and DMF. However, for arrays where BODIPY is attached through a phenylacetylene linker at the 3- and 3,13-positions, quantum yields depend on the solvent, and fluorescence is diminished in DMF, compared to toluene. While reduction of fluorescence in the case of **2-(BDP)$_2$** (0.93-fold in DMF, compared to toluene) is comparable with these observed for amide-linker dyads, a more pronounced reduction in intensity is observed for **1-BDP**, (0.71-fold intensity in DMF of that in toluene), and almost complete quenching (∼30 times) for **Zn2-(BDP)$_2$**. The observed reduction of fluorescence in polar DMF is most likely due to photoinduced electron transfer (PET) from excited chlorin to BODIPY. Such PET would be more favorable in polar solvents, due to the stabilization of the resulting ion-radical pair. The much more extensive quenching of fluorescence observed for **Zn2-(BDP)$_2$** can be explained by the lower oxidation potential for zinc complexes of chlorins, compared to the corresponding free bases;[18] hence, the chlorin moiety in **Zn2-(BDP)$_2$** is likely more prone to oxidation than in **2-(BDP)$_2$**. Similarly, it has been reported that installation of (phenyl)ethynyl substituents at the 3,13-positions of chlorin leads to the increase of the oxidation potential of chlorin;[4,18] thus, this explains the lower fluorescence for **1-BDP** vs **2-(BDP)$_2$** in DMF.

The important observation is that fluorescence quantum yields for amide-linked dyads are nearly identical in DMF and toluene. Particularly striking is the difference between **Zn2-(BDP)$_2$** and **Zn4-BDP**, where chlorin macrocycles should possess comparable redox properties. The nearly complete quenching of fluorescence for **Zn2-(BDP)$_2$** in DMF and no quenching for **Zn4-BDP** indicate that the type of linker connecting the chlorin and BODIPY and perhaps the position of BODIPY attachment play a critical role in photochemical properties of resulting arrays. A possible reason for the observed differences might be the stronger electronic coupling between chlorin and BODIPY in phenylethynyl-linked dyads

DOI: 10.1021/acs.joc.5b00119
J. Org. Chem. 2015, 80, 3858−3869

1-BDP and **(Zn)2-(BDP)$_2$**, which facilitates electron transfer from photoexcited chlorin to BODIPY. It is known that phenylethynyl-type linkers provide strong electronic coupling between dyads' components and promote ultrafast PET.[39] Electronic communication between BODIPY and chlorin can be inferred from absorption and emission spectra of **1-BDP** and **(Zn)2-(BDP)$_2$**, which show slight bathochromic shift of both Q_y absorption and emission bands, and increased fluorescence quantum yields (in toluene) of chlorin components, compared to the benchmark monomers (see Table 1). For **3-BDP** and **4-BDP**, both absorption and emission maxima and fluorescence quantum yields are identical to those for the corresponding benchmark monomers, which suggests that there is a negligible conjugation between chlorin and BODIPY, which, in turn, may lead to an attenuation of photoinduced electron transfer. However, further systematic time-resolved spectroscopic and electrochemical measurements are necessary to elucidate the exact mechanism of quenching of fluorescence for chlorin components in arrays.

In order to further evaluate the applicability of amide-linked BODIPY−chlorin dyads for bioimaging, we compared the quantum yields of fluorescence for the chlorin component in arrays upon excitation at the maximum of the BODIPY absorption, in various solvents (toluene, MeOH, DMSO, DMF; Table S1, Supporting Information). The data show that the dyads **3-BDP**, **4-BDP**, and **Zn4-BDP** retain relatively high fluorescence quantum yields in solvents of different polarities. Fluorescence for these arrays is comparable in toluene, DMF, and DMSO, and modestly reduced in MeOH (on average fluorescence quantum yields in MeOH are 0.71-fold of that in toluene). Finally, we compared the fluorescence intensity for dyads vs monomers upon excitation at ∼500 nm, at the same concentration. We observed 5.2-fold and 4.7-fold increases for **3-BDP** and 5.5-fold and 5.2-fold for **4-BDP** in toluene and DMF, respectively.

■ CONCLUSION AND OUTLOOK

We identified the molecular architecture for BODIPY−chlorin arrays with bright fluorescence of chlorin upon excitation at ∼500 nm in various solvents of different polarities. While all examined arrays exhibit an efficient energy transfer from BODIPY to the chlorin moiety, the dyads where BODIPY is attached at 13- or 3,13-positions of chlorin exhibit diminished fluorescence in polar solvent, compared to that observed in toluene. The reduction of fluorescence is the most pronounced in the case of the array comprising a Zn(II) complex of chlorin. On the contrary, dyads where BODIPY is attached through an amide bond at the 10-position of chlorin exhibit a relatively high fluorescence quantum yield in various solvents of different polarities, for all three dyads examined. Therefore, the construct, represented by dyads **3-BDP** and **(Zn)4-BDP**, constitutes an attractive platform for development of deep-red or near-IR fluorophores excitable with green (and near-IR) light. In that architecture, the wavelength of chlorin emission can be tuned by placing different substituents at 3,13-positions of chlorin, or by insertion of Zn(II) into the chlorin macrocycle. Obviously, application of reported dyads in fluorescence imaging requires modification of their structure to provide water solubility, installation of bioconjugatable groups, etc. These are the subjects of ongoing research in our laboratory.

■ EXPERIMENTAL SECTION

General Experimental Section. ^{1}H NMR (400 MHz), ^{13}C NMR (100 MHz), and ^{19}F NMR (376 MHz) spectra were collected at room temperature in $CDCl_3$, unless noted otherwise. Chemical shifts (δ) were callibrated using solvent peaks (^{1}H signals: residual proton signals: 7.26 ppm for chloroform, 2.50 ppm for DMSO; ^{13}C signals: 77.0 ppm for $CDCl_3$, 39.5 ppm for DMSO-d_6). All solvents and commercially available reagents were used as received. Palladium coupling reactions was performed using commercially available anhydrous solvents (toluene and DMF). Low-resolution LD-MS analyses were performed without matrix. The FT-ICR analyzer was used for ESI and MALDI HRMS.

Known compounds **1-Br**,[20] **5**,[20] **7**,[40] **BDP-NH$_2$**,[36] and **7-Br**[41] were prepared following reported procedures. Known compound **6-Br$_2$**,[20] **BDP-TMS**,[34] and **BDP-H**,[34] were prepared by modified procedure.

3,13-Dibromo-18,18-dimethyl-10-(4-methoxycarbonylphenyl)-chlorin (2-Br$_2$). Following a reported precedure,[32,33] a solution of **5** (610 mg, 2.00 mmol) in THF (20 mL) and treated with NBS (696 mg, 4.00 mmol) under nitrogen at −78 °C. The resulting reaction mixture was stirred for 1 h at −78 °C. The cooling bath was removed, the reaction mixture was warmed up to −20 °C, and a hexanes/water mixture (∼10 mL, 1:1) was added. The organic layer was separated, dried (Na_2SO_4), and concentrated. Column chromatography (silica [hexanes/dichloromethane/ethyl acetate, 7:3:2]) provided a white/pale yellow solid (0.62 g, 67%). The resulting **6-Br$_2$** was immediately used in the next step without further characterization.

Following a reported precedure,[32,33] a mixture of **6-Br$_2$** (0.516 g, 1.14 mmol) and **7-Br**[40] (0.315 g, 1.14 mmol) in CH_2Cl_2 (30 mL) was treated with a solution of *p*-toluenesulfonic acid (1.26 g, 6.65 mmol) in MeOH (10 mL). The resulting mixture was stirred at room temperature for 30 min. A sample of 2,2,6,6-tetramethylpiperidine (6.65 mL, 38.6 mmol) was added to the reaction flask, and the resulting mixture was concentrated. The resulting orange-red solid was suspended in acetonitrile (100 mL) and treated with $Zn(AOc)_2$ (3.66 g, 20.0 mmol), AgOTf (1.0 g, 4.0 mmol), and (TMP (6.78 mL, 39.9 mmol). The resulting mixture was refluxed overnight and then concentrated. The crude zinc complex of chlorin was filtered through silica (CH_2Cl_2), and all green fractions containing chlorin were collected and concentrated. The resulting solid was dissolved in dichloromethane (10 mL), treated with TFA (1.00 mL), and stirred for 4 h. Saturated aqueous $NaHCO_3$ was added and stirred for 5 min. The organic layer was separated, washed (water and brine), dried (Na_2SO_4), and concentrated, to give a red-brown solid. Column chromatography [silica, hexane/CH_2Cl_2 (1:1)] provided a dark-green solid (125 mg, 17%). ^{1}H NMR δ −2.17 (s, 1H), −1.78 (s, 1H), 2.04 (s, 6H), 4.13 (s, 3H), 4.63 (s, 2H), 8.18 (d, J = 8.0 Hz, 2H), 8.43 (d, J = 8.0 Hz, 2H), 8.50 (d, J = 4.0 Hz, 1H), 8.76 (s, 1H), 8.78 (s, 1H), 8.94 (d, J = 4.0 Hz, 1H), 8.96 (s, 1H), 9.15(s, 1H), 9.85 (s, 1H); ^{13}C NMR δ 31.2, 46.5, 52.1, 52.6, 94.8, 95.7, 105.9, 113.8, 118.8, 120.2, 124.7, 128.3, 128.7, 129.9, 132.2, 132.4, 133.3, 134.0, 134.1, 137.2, 140.2, 145.9, 151.2, 152.4, 163.7, 167.4, 176.0; MS m/z $[M + H]^+$ Calcd for $C_{30}H_{25}N_4O_2Br_2$ 631.0339; Found (HRMS-ESI) 631.03117.

9-Bromo-1-formyl-5-(4-methoxycarbonylphenyl)dipyrromethane (6-Br). Following a reported procedure,[32] a solution of **5**[20] (1.08 g, 3.51 mmol) in THF (60 mL) was treated with NBS (0.640 g, 3.60 mmol) at −78 °C. After 40 min, the cooling bath was removed, and a mixture of hexane and water (1:1, 10 mL) was added. The resulting mixture was diluted with ethyl acetate, washed with brine, and dried (Na_2SO_4) and concentrated. Column chromatography [silica, hexane/ethyl acetate (2:1)] provided the desired product as a white powder (1.27 g, 94%): ^{1}H NMR (DMSO-d_6) δ 3.83 (s, 3 H), 5.54 (s, 1H), 5.67 (app t, J = 3.0 Hz, 1H), 6.01−5.93 (m, 2H), 6.91 (app t, J = 3.0 Hz, 1H), 7.28 (d, J = 8.2 Hz, 2H), 7.90 (d, J = 8.2 Hz, 2H), 9.39 (s, 1H), 11.46 (br, 1H), 12.09 (br, 1H). The product was used immediately in the next step without further characterization.

10-(4-Methoxycarbonylphenyl)-18,18-dimethylchlorin (3). Following a reported procedure,[32] a suspension of **7**[40] (0.620 g, 3.26 mmol) and **6-Br** (1.27 g, 3.28 mmol) in dichloromethane (80 mL) was treated with a solution of *p*-toluenesulfonic acid (3.04 g, 16.0 mmol) in methanol (20 mL) and stirred at room temperature for 40 min. The resulting mixture was treated with 2,2,6,6-tetramethylpiperidine

DOI: 10.1021/acs.joc.5b00119
J. Org. Chem. 2015, 80, 3858−3869

(6.60 mL, 38.9 mmol). The reaction mixture was concentrated, and the resulting brown solid was suspended in acetonitrile (300 mL) and treated with zinc acetate (8.78 g, 48.0 mmol), 2,2,6,6-tetramethylpiperidine (13.5 mL, 79.5 mmol), and AgOTf (2.50 g, 9.73 mmol). The resulting suspension was refluxed for 17 h. The reaction mixture was cooled down and concentrated, and the residue was purified by column chromatography [silica, hexanes/dichloromethane (1:2)]. The resulting green solid (crude zinc chlorin) was treated with a solution of TFA (5.80 mL, 75.3 mmol) in CH_2Cl_2 (70 mL). The resulting mixture was stirred for 3 h, then washed (saturated aqueous $NaHCO_3$ and brine), dried (Na_2SO_4), and concentrated. Column chromatography [silica, hexanes/CH_2Cl_2 (1:2)] provided a green solid (0.422 g, 25%): ^{1}H NMR δ −2.34 (s, 1H), −1.96 (s, 1H), 2.07 (s, 6H), 4.13 (s, 3H), 4.64 (s, 2H), 8.27 (d, J = 8.3 Hz, 2H), 8.45 (d, J = 8.3 Hz, 2H), 8.62 (d, J = 4.3 Hz, 1H), 8.78 (d, J = 4.9 Hz, 1H), 8.85 (d, J = 4.3 Hz, 1H), 8.96 (s, 1H), 8.98 (d, J = 4.9 Hz, 1H), 9.01 (d, J = 4.3 Hz, 1H), 9.05 (s, 1H), 9.26 (d, J = 4.9 Hz, 1H), 9.89 (s, 1H); ^{13}C NMR δ 31.2, 46.4, 52.0, 52.4, 94.5, 97.1, 107.3, 119.9, 123.4, 123.8, 127.8, 128.0, 128.4, 129.4, 131.6, 132.6, 134.1, 134.3, 134.7, 139.4, 140.9, 146.6, 150.9, 151.8, 163.0, 167.4, 175.4; HRMS (ESI) m/z [M + H]$^+$ Calcd for $C_{30}H_{26}N_4O_2$ 475.2129; Found 475.2118.

8-[4-(Trimethylsilyl)ethynylphenyl)]-4,4-difluoro-1,3,5,7-tetramethyl-4-bora-3a,4a-diaza-*s*-indacene (BDP-TMS).[34] A mixture of 4-[(trimethylsilyl)ethynyl]benzaldehyde (0.404 g, 2.00 mmol) and 2,4-dimethylpyrrole (0.440 g, 4.00 mmol) in anhydrous dichloromethane (100 mL) was treated with trifluoroacetic acid (15 μL, 0.2 mmol), and the reaction mixture was stirred at room temperature for 6 h, under N_2 to obtain a deep-red mixture. A sample of DDQ (0.454 g, 2.00 mmol) was added, and the resulting mixture was stirred for 1 h. Samples of NEt_3 (3.40 g, 33.6 mmol) and $BF_3{\cdot}OEt_2$ (5.20 g, 36.6 mmol) were then added, and the resulting mixture was stirred overnight. The mixture was washed with saturated aqueous $NaHCO_3$, dried (Na_2SO_4), and concentrated. A viscous oily liquid was obtained. Column chromatography [silica, hexane/ethyl acetate (20:1)] provided a solid, which was washed with hexanes, and dried under vacuum to obtain an orange solid, (196 mg, 23%). ^{1}H NMR δ 0.28 (s, 9H), 1.40 (s, 6H), 2.56 (6H), 5.98 (s, 2H), 7.25 (d, J = 8.2 Hz, 2H, overlap with $CHCl_3$ peak), 7.61 (d, J = 8.2 Hz, 2H); ^{13}C NMR δ (100 MHz): 0.01, 14.7, 95.9, 100.0, 104.3, 121.5, 124.0, 128.2, 131.3, 132.8, 135.3, 140.9, 143.1, 155.9; ^{19}F NMR δ −146.1 (q, J = 34.0 Hz); MS m/z [M + H]$^+$ Calcd for $C_{24}H_{27}BF_2N_2Si$ 421.2082; Found (LD-MS) 421.6, (HRMS-ESI) 421.2094.

8-(4-Ethynylphenyl)-4,4-difluoro-1,3,5,7-tetramethyl-4-bora-3a,4a-diaza-*s*-indacene BDP-H.[34] A mixture of **BDP-TMS** (0.558 g, 1.33 mmol) and potassium carbonate (0.201 g, 1.459 mmol) in methanol/THF (1:1, 66 mL) was stirred for 1 h, after which water was added to the mixture. The mixture was extracted thrice with dichloromethane. The organic extracts were concentrated, and the remaining solid was dried under high vacuum. The dried compound was chromatographed [silica, hexane/ethyl acetate (15:1)] to obtain an orange solid (0.278 g, 60%). ^{1}H NMR δ 1.39 (s, 6H), 3.17 (s, 1H), 5.98 (s, 2H), 7.26 (d, J = 8.3 Hz, 2H, overlaps with $CHCl_3$ peak), 7.62 (d, J = 8.2 Hz, 2H); ^{13}C NMR δ 14.65, 14.69, 78.7, 83.0, 121.5, 123.1, 128.3, 131.2, 133.0, 135.7, 140.7, 143.1, 155.9; MS m/z [M + H]$^+$ Calcd for $C_{21}H_{19}BF_2N_2$ 349.1682; Found: (LD-MS) 349.2, (HRMS-ESI) 349.1683.

1-BDP. Following a reported procedure,[35] a mixture of **1-Br** (20 mg, 0.036 mmol) and **BDP-H** (15 mg, 0.043 mmol) in DMF/triethylamine (2:1, 6 mL) was degassed by freeze−thaw cycles (two times). A sample of $(PPh_3)_2PdCl_2$ (3.8 mg, 0.0054 mmol) was added under nitrogen. The resulting mixture was degassed using a freeze−thaw cycle under nitrogen. The reaction flask was placed in an oil bath preheated to 80 °C. After 2 h, TLC [silica, hexanes/CH_2Cl_2 (1:1)] showed a complete consumption of the starting chlorin. The reaction mixture was diluted with ethyl acetate, washed (water and brine), dried (Na_2CO_3), and concentrated. Column chromatography [silica, hexane/CH_2Cl_2 (1:2)] provides a brown solid (which appears green in solution and on the chromatography column). Yield: 15 mg, 52%. ^{1}H NMR δ −2.07 (br, 1H), −1.64 (br, 1H), 1.55 (s, 6H), 2.08 (s, 6H), 2.60 (s, 6H), 4.11 (s, 3H), 4.71 (s, 2H), 6.04 (s, 2H), 7.44 (d, J = 8.3 Hz, 2H), 8.00 (d, J = 8.2 Hz, 2H), 8.24 (d, J = 8.7 Hz, 2H), 8.43 (d, J = 8.2 Hz, 2H), 8.58 (d, J = 4.1 Hz, 1H), 8.91−8.97 (m, 4H), 9.23 (d, J = 4.6 Hz, 1H), 9.37 (s, 1H), 9.80 (s, 1H); ^{13}C NMR δ 14.3, 14.9, 31.2, 46.8, 52.1, 52.6, 86.0, 95.0, 95.5, 96.0, 107.3, 116.7, 124.4, 124.5, 128.3, 128.6, 129.2, 129.5, 129.8, 131.4, 132.5, 132.6, 133.0, 133.2, 134.2, 135.42, 135.44, 139.6, 141.9, 143.2, 146.3, 152.1, 152.2, 156.0, 163.6, 167.4, 176.7; ^{19}F NMR δ −146.1 (q, J = 30.9 Hz); MS m/z [M + H]$^+$ Calcd for $C_{51}H_{43}BF_2N_6O_2$ 821.3589; Found (LD-MS) 821.8, (HRMS-ESI) 821.3597.

2-BDP. Following a reported precedure,[35] a mixture of **2-Br$_2$** (10 mg, 0.016 mmol) and **BDP-H** (14 mg, 0.040 mmol) in DMF/Et_3N (6 mL, 2:1) was degassed by freeze/thaw (2 cycles). Then, a sample of $(PPh_3)_2PdCl_2$ (1.5 mg, 0.0021 mmol) was added, and the mixture was degassed by one more freeze/thaw cycle. The reaction mixture was placed in a preheated oil bath, and stirred at 80 °C for 3 h. The resulting mixture was diluted with water and extracted with ethyl acetate, and the organic phase was washed (water, brine), dried (Na_2SO_4), and concentrated. Column chromatography (silica, hexanes/dichloromethane 1:1 → 1:10) provided a brown solid, which was washed with methanol and hexanes (9.1 mg, 47%). ^{1}H NMR δ −1.88 (br, 1H), −1.45 (br, 1H), 1.55, 1.58 (two singlets overlapped with water signal), 2.09 (s, 6H), 2.60−2.61 (broad, two overlapped singlets, 12H), 4.12 (s, 3H), 4.71 (s, 2H), 6.05, 6.06 (two overlapped singlets, 4H), 7.46 (d, J = 7.3 Hz, 2H), 7.51 (d, J = 7.3 Hz, 2H), 8.00 (d, J = 7.3 Hz, 2H), 8.12 (d, J = 7.3 Hz, 2H), 8.24 (d, J = 8.2 Hz, 2H), 8.44 (d, J = 8.2 Hz), 8.58 (d, J = 4.1 Hz, 1H), 8.87 (s, 1H), 8.89 (s, 1H), 9.02 (d, J = 4.1 Hz, 1H), 9.35 (s, 1H), 10.07 (s, 1H); MS m/z [M]$^+$ Calcd for $C_{72}H_{60}B_2F_4N_8O_2$ 1167.49995; Found (HRMS-MALDI) 1167.5024.

Zn2-(BDP)$_2$. A mixture of **2-(BDP)$_2$** (3.5 mg, 0.0036 mmol) in $CHCl_3$/MeOH (1 mL, 5:1) was treated with $Zn(OAc)_2$ (10 mg, 0.055 mmol) and stirred at 50 °C for 1 h. The reaction mixture was concentrated (^{1}H NMR was recorded at this point). The sample was then dissolved in CH_2Cl_2, washed (water and brine), dried (Na_2SO_4), and concentrated. The resulting solid was washed with MeOH and hexanes (with sonication), to provide a green solid (3.6 mg, 97%). The product, after washing with water, MeOH, and hexanes, showed extremely low solubility in common organic solvents ($CHCl_3$, CH_2Cl_2, THF, DMSO), which prevents recording a ^{1}H NMR spectrum of the pure sample. The ^{1}H NMR data reported here were taken on the semipure sample, before washing with water, MeOH, and hexanes. ^{1}H NMR δ 1.54 (s, 6H), 1.58 (s, 6H), 2.07 (s, 6H), 2.59 (broad, two overlapped singlets, 12H), 4.10 (s, 3H), 4.62 (s, 2H), 6.04 and 6.05 (two overlapped singlets, 4H), 7.43 (d, J = 8.1 Hz, 2H), 7.49 (d, J = 8.1 Hz, 2H), 7.96 (d, J = 8.1 Hz, 2H), 8.09 (d, J = 8.1 Hz, 2H), 8.18 (d, J = 8.1 Hz, 2H), 8.40 (d, J = 8.1 Hz, 2H), 8.50 (d, J = 4.2 Hz, 1H), 8.63 (s, 1H), 8.80 (s, 1H), 8.96 (s, 1H), 8.96 (d, J = 4.2 Hz, 1H), 9.10 (s, 1H), 9.93 (s, 1H); MS m/z [M]$^+$ Calcd for $C_{72}H_{58}B_2F_4N_8O_2Zn$ 1228.4113; Found (LD-MS) 1228.3 (HRMS MALDI) 1228.4092.

3-BDP. Following a reported precedure,[20] a solution of **3** (118 mg, 0.249 mmol) in THF (4 mL) and methanol (2 mL) was treated with NaOH (1 M aqueous solution, 2 mL) and stirred under nitrogen for 14 h. The reaction mixture was treated with aqueous HCl solution (1M, 10 mL) and extracted with CH_2Cl_2. Combined organic layers were dried over anhydrous Na_2SO_4 and concentrated to afford an intermediate acid **3-COOH** as a green powder (112 mg, 98%), which was used in the next step without further purification: ^{1}H NMR (DMSO-d_6) δ −2.56 (s, 1H), −2.12 (s, 1H), 2.02 (s, 6H), 4.63 (s, 2H), 8.24 (d, J = 8.3 Hz, 2H), 8.37 (d, J = 8.3 Hz, 2H), 8.49 (d, J = 4.3 Hz, 1H), 8.78 (d, J = 4.9 Hz, 1H), 9.13−9.06 (m, 2H), 9.28−9.20 (m, 3H), 9.50 (d, J = 4.2 Hz, 1H), 10.08 (s, 1H), 13.27 (br, 1H); ^{13}C NMR (DMSO-d_6) δ 30.8, 46.2, 51.3, 94.8, 97.3, 107.4, 119.4, 124.1, 124.7, 127.7, 128.9, 129.1, 130.2, 131.2, 133.1, 133.8, 134.0, 134.1, 138.9, 140.7, 145.4, 150.3, 151.0, 163.6, 167.6, 175.7; HRMS (ESI) m/z [M + H]$^+$ Calcd for $C_{29}H_{24}N_4O_2$ 461.1972; Found 461.1972.

A solution of **BDP-NH$_2$**[36] (14.7 mg, 0.0434 mmol) in DMF (5 mL) was treated with crude **3-COOH** (20.0 mg, 0.0434 mmol), EDC hydrochloride (83.0 mg 0.434 mmol), and DMAP (5.3 mg, 0.043 mmol) and was stirred at room temperature overnight. The resulting mixture was diluted with ethyl acetate (20 mL), and the organic layer

DOI: 10.1021/acs.joc.5b00119
J. Org. Chem. 2015, 80, 3858−3869

was then washed with water and brine, dried (Na_2SO_4), and concentrated. Column chromatography [silica, hexane/CH_2Cl_2 (1:2)] provided a brown-green solid; 18.0 mg, 53%. ^{1}H NMR δ −2.37 (bs, 1H), −1.98 (bs, 1 H), 1.54 (s, 6H), 2.09 (s, 6H), 2.59 (s, 6H), 4.68 (s, 2H), 6.03 (s, 2H), 7.39 (d, J = 8.4 Hz, 2H), 7.99 (d, J = 8.4, 2H), 8.25 (s, 1H), 8.28 (d, J = 8.2 Hz, 2H), 8.33 (d, J = 8.2 Hz, 2H), 8.61 (d, J = 4.3 Hz, 1H), 8.79 (d, J = 4.7 Hz, 1H), 8.89 (d, J = 4.7 Hz, 1H), 9.00 (d, J = 4.3 Hz, 1H), 8.97 (s, 1H), 9.02 (d, J = 4.4 Hz, 1H), 9.10 (s, 1H), 9.29 (d, J = 4.3, 1H), 9.91 (s, 1H); ^{13}C NMR δ 14.6, 14.8, 31.2, 46.5, 52.0, 94.6, 97.2, 107.4, 119.5, 120.4, 121.3, 123.5, 123.9, 125.5, 127.7, 128.5, 129.0, 131.0, 131.5, 131.6, 132.7, 133.8, 134.3, 134.5, 134.7, 138.9, 139.4, 141.0, 141.2, 143.1, 146.0, 150.9, 151.8, 155.6, 163.2, 165.9, 175.5; ^{19}F NMR δ −146.1 (q, J = 33.4 Hz); HRMS (ESI) m/z [M + H]$^+$ Calcd for $C_{48}H_{42}BF_2N_7O$ 782.359; Found 782.3574.

4-BDP. Following a reported precedure,[20] a sample of **2** (41.7 mg, 0.0617 mmol) was dissolved in THF (4 mL) and methanol (3 mL) and treated with aqueous NaOH (3 mL, 1.0 M). After 20 h ,TLC (dichloromethane) showed consumption of all starting material and a single, more polar, red fluorescent spot. The reaction mixture was diluted with dichloromethane (15 mL), quenched with HCl (~3 mL, 1M), washed with water and brine, dried (Na_2SO_4), and concentrated. ^{1}H NMR clearly indicated the loss of the methoxy group. The yield of hydrolysis was assumed to be quantitative, and the resulting acid **2-COOH** was used in the next step without further purification. ^{1}H NMR δ 2.08 (s, 3H), 4.69 (s, 2H), 7.49−7.59 (m, 8H), 7.88−7.90 (m, 2H), 7.98−8.00 (m, 2H), 8.29 (d, J = 8.2 Hz, 2H), 8.53 (d, J = 8.2 Hz, 2H), 8.58 (d, J = 4.4 Hz, 1H), 8.86 (s, 1H), 8.88 (s, 1H), 9.02 (d, J = 4.4 Hz, 1H), 9.05 (s, 1H), 9.35 (s, 1H), 10.07 (s, 1H).

Following a reported precedure,[20] a solution of **BDP-NH$_2$**[36] (18.0 mg, 0.0530 mmol) in DMF (7 mL) was treated with **2-COOH** (35.0 mg, 0.0530 mmol), EDC hydrochloride (101 mg, 0.530 mmol), and DMAP (6.5 mg, 0.053 mmol) and was stirred at room temperature overnight. The resulting mixture was diluted with ethyl acetate (20 mL), and the organic layer was then washed with water and brine, dried (Na_2SO_4), and concentrated. Column chromatography [silica, hexane/CH_2Cl_2 (1:2)] yielded a mixture of product and a green-fluorescent impurity. The resulting sample was dissolved in CH_2Cl_2, mixed with silica (~2g), and concentrated. The resulting powder was loaded on the top of a silica column and eluted with MeOH (the green-fluorescent impurity was eluted, whereas insoluble **4-BDP** stayed on the top of the column). Elution with MeOH was continued until the green-fluorescent impurity was completely eluted. The **4-BDP** was then eluted with CH_2Cl_2. The resulting sample was washed with MeOH and hexanes to afford a brown solid. 13.1 mg, 25%. ^{1}H NMR δ −1.92 (bs 1H) −1.50 (bs, 1H), 1.55 (s, 6H), 2.08 (s, 6H), 2.59 (s, 6H), 4.69 (s, 2H), 6.03 (s, 2H), 7.40 (d, J = 8.5 Hz, 2H), 7.59−7.48 (m, 7H), 7.42−7.38 (m, 2H), 8.00−7.95 (m, 3H), 8.2 (s, 1H) 8.33−8.27 (m, 4H), 8.58 (d, J = 4.3 Hz, 1H), 8.86 (s, 1H), 8.87 (s, 1H), 9.02 (d, J = 4.4 Hz, 1H), 9.05 (s, 1H), 9.34 (s, 1H), 10.07 (s, 1H); ^{13}C NMR δ 14.6, 14.7, 31.1, 46.4, 52.1, 84.0, 84.1, 95.2, 95.8, 97.1, 98.1, 105.4, 118.2, 120.0, 120.4, 121.3, 122.9, 123.2, 123.3, 125.2, 125.7, 128.6, 128.7, 128.8, 128.9, 129.0, 129.4, 131.0, 131.6, 131.8, 132.0, 132.1, 133.4, 134.0, 134.1, 134.5, 135.4, 138.9, 140.0, 140.1, 141.2, 143.1, 145.3, 151.8, 152.6, 155.6, 164.1, 165.8, 176.1; ^{19}F NMR δ −146.1 (q, J = 33.1 Hz); HRMS (ESI) m/z [M + H]$^+$ Calcd for $C_{64}H_{50}BF_2N_7O$ 982.4221; Found 982.4193.

Zn4-BDP. A sample of **4-BDP** (4.7 mg, 0.048 mmol) was dissolved in chloroform (2.5 mL) and methanol (0.5 mL) and treated with zinc acetate (1.9 mg, 0.010 mmol). After 6 h, TLC indicated that all starting material had been consumed. The reaction mixture was then quenched with saturated aqueous $NaHCO_3$, washed with water and brine, dried (Na_2SO_4), and concentrated. Column chromatography [silica, CH_2Cl_2] provided a green solid that became brown after extensive drying 3.0 mg, 57%. ^{1}H NMR δ 1.53 (s, 6H, overlapped with water signal), 2.06 (s, 6H), 2.59 (s, 6H), 4.59 (s, 2H), 6.03 (s, 2H), 7.37 (d, J = 8.4 Hz, 2H), 7.55−7.40 (m, 6H), 7.81 (d, J = 7.0 Hz, 2H), 7.85 (d, J = 7.7 Hz, 2H), 7.92 (d, J = 6.8 Hz, 2H), 8.10 (d, J = 7.5 Hz, 2H), 8.24−8.15 (m, 3H), 8.47 (d, J = 4.2 Hz, 1H), 8.60 (s, 1H), 8.77 (s, 1H), 8.91 (s, 1H), 8.92 (d, J = 4.0 Hz, 1H), 9.07 (s, 1H), 9.87 (s, 1H); MS m/z [M + H]$^+$ Calcd for $C_{64}H_{48}BF_2N_7OZn$ 1043.32777; Found (LD-MS) 1042.9 (HRMS-MALDI) 1043.3265.

18,18-Dimethyl-10-(4-methoxycarbonylphenyl)-13-phenylethynylchlorin (1). Following a reported precedure,[35] a solution of **1-Br**[20] (15.2 mg, 0.0275 mmol), in DMF/Et_3N (6 mL, 2:1) was degassed by freeze/thaw (2 cycles), and a sample of $(PPh_3)_2PdCl_2$ (3 mg, 0.004 mmol) was added, and the mixture was degassed by one more freeze/thaw cycle. A sample of phenylacetylene (5.6 μL, 0.052 mmol), and the resulting mixture was stirred at 80 °C for 3 h. The reaction mixture was dilluted with water and extracted with ethyl acetate. The organic phase was washed (water and brine), dried (Na_2SO_4), and concentrated. Column chromatography (silica, hexanes/dichloromethane, 1:2) provided a green solid; 13 mg, 84%: ^{1}H NMR δ −2.11 (br, 1H), −1.72 (br, 1H), 2.08 (s, 6H), 4.12 (s, 3H), 4.70 (s, 2H), 7.45−7.54 (m, 3H), 7.87−7.89 (m, 2H), 8.24 (d, J = 8.2 Hz, 2H), 8.43 (d, J = 8.2 Hz, 2H), 8.58 (d, J = 4.3 Hz, 1H), 8.88 (s, 1H), 8.91 (s, 1H), 8.94 (d, J = 4.4 Hz, 1H), 8.96 (d, J = 4.3 Hz, 1H), 9.22 (d, J = 4.4 Hz, 1H), 9.38 (s, 1H), 9.81 (s, 1H); ^{13}C NMR δ 31.2, 46.8, 52.2, 52.6, 95.0, 95.6, 96.8, 107.3, 117.5, 120.6, 123.6, 124.2, 128.3, 128.76, 128.81, 129.0, 129.3, 129.7, 132.0, 132.3, 132.9, 133.3, 134.2, 135.2, 139.7, 141.7, 146.3, 151.9, 152.1, 163.7, 167.5, 176.4; HRMS (MALDI) m/z [M + H]$^+$ Calcd for $C_{38}H_{30}N_4O_2$ 575.2442; Found 575.2451.

18,18-Dimethyl-10-(4-methoxycarbonylphenyl)-3,13-diphenylethynylchlorin (2). Following a reported precedure,[35] a mixture of **2-Br$_2$** (20 mg, 0.030 mmol) and $(PPh_3)_2PdCl_2$ (2.1 mg, 0.0030 mmol, 10 mol %) in DMF/NEt_3 (9 mL, 2:1) was placed in a Schlenk flask. The mixture was deoxygenated by freeze−pump−thaw cycles (3 times), and a sample of phenylacetylene (0.013 mL, 0.012 mmol) was added to the reaction flask. The reaction mixture was stirred for 4 h at 80 °C. The resulting mixture was washed (water and brine), dried (Na_2SO_4), and concentrated to obtain a dark brown solid. Column chromatography [silica, hexane/ethyl acetate (5:1)] provided a brown solid (12 mg, 60%). ^{1}H NMR δ −1.93 (s, 1H), −1.50 (s, 1H), 2.07 (s, 6H), 4.11 (s, 3H), 4.68 (s, 2H), 7.52(m, 6H), 7.87 (d, J = 8.0 Hz, 2H), 7.99 (d, J = 8.0 Hz, 2H), 8.24 (d, J = 12 Hz, 2H), 8.43 (d, J = 8 Hz, 2H), 8.55 (d, J = 4 Hz, 1H), 8.85 (s, 2H, 2 signal overlap), 9.00 (d, J = 4 Hz, 1H), 9.04 (s, 1H), 9.33 (s, 1H) ; ^{13}C NMR δ 31.3, 46.6, 52.3, 52.6, 84.2, 84.4, 95.3, 95.9, 97.2, 98.2, 105.6, 118.3, 120.6, 123.0, 123.4, 123.4, 125.3, 128.4, 128.8, 128.9, 129.0, 129.2, 129.7, 129.8, 132.0, 132.2, 132.5, 133.6, 134.2, 134.3, 135.6, 140.2, 146.2, 152.0, 152.9, 164.2, 167.5, 176.2; MS m/z [M + H]$^+$ Calcd for $C_{46}H_{35}N_4O_2$ 675.2754; Found (HRMS-ESI) 675.2780, (MALDI-MS) 674.7.

18,18-Dimethyl-10-(4-methoxycarbonylphenyl)-3,13-diphenylethynylchlorinato Zinc(II) (Zn2). A solution of **2** (15.0 mg, 0.0222 mmol) in $CHCl_3$/MeOH (6 mL, 5:1) was treated with $Zn(OAc)_2$ (8.2 mg, 0.045 mmol). The resulting mixture was stirred at 50 °C for 30 min. The reaction mixture was diluted with water, and the resulting mixture was extracted with ethyl acetate. Combined organic phases were washed (water and brine), dried (Na_2SO_4), and concentrated. Column chromatography [silica, hexanes/CH_2Cl_2 1:3] provided a green solid, which was washed (with sonication) with hexanes and MeOH; 12.1 mg, 71%). ^{1}H NMR δ 2.05 (s, 6H), 4.08 (s, 3H), 4.58 (s, 2H), 7.55−7.43 (m, 6H), 7.82 (d, J = 7.0 Hz, 2H), 7.94 (d, J = 7.0 Hz, 2H), 8.16 (d, J = 8.0 Hz, 2H), 8.37 (d, J = 8.0, 2H), 8.46 (d, J = 4.2 Hz, 1H), 8.57 (s, 1H), 8.74 (s, 1H), 8.88 (s, 1H), 8.90 (d, J = 4.2 Hz, 1H), 9.05 (s, 1H), 9.85 (s, 1H); HRMS (MALDI) m/z [M]$^+$ Calcd for $C_{46}H_{32}N_4O_2Zn$ 736.1811; Found 736.1819.

8-(4-benzamidophenyl)-4,4-difluoro-1,3,5,7-tetramethyl-4-bora-3a,4a-diaza-*s*-indacene (BDP-NHBz). A solution of **BDP-NH$_2$**[36] (0.020 g, 0.059 mmol) in DMF (10 mL) was treated with benzoic acid (0.072 g, 0.590 mmol), EDC hydrochloride (0.0226 g, 0.118 mmol), and DMAP (0.0144 g, 0.118 mmol) and was stirred at room temperature. After 40 h, the resulting mixture was diluted with ethyl acetate (20 mL), and the organic layer was washed with water and brine, dried (Na_2SO_4), and concentrated. Column chromatography [silica, CH_2Cl_2/hexane/ethyl acetate (20:1:1)] provided a semipure compound. Subsequent column chromatography (silica, CH_2Cl_2) provided a bright orange-red solid; 20.8 mg, 80%. ^{1}H NMR δ 1.46 (s, 6H), 2.56 (s, 6H), 5.99 (s, 2H), 7.30 (d, J = 8.4 Hz, 2H),

DOI: 10.1021/acs.joc.5b00119
J. Org. Chem. 2015, 80, 3858−3869

7.56−7.50 (m, 2H), 7.62−7.57 (m, 1H), 7.82 (d, J = 8.4 Hz, 2H), 7.94−7.89 (m, 3H); ^{13}C NMR δ 14.6, 14.7, 120.2, 121.2, 127.0, 128.9, 128.9, 130.9, 131.6, 132.2, 134.6, 138.7, 141.1, 143.1, 155.5, 165.8; ^{19}F NMR δ −146.2 (q, J = 33.7 Hz); HRMS (ESI) m/z $[M + H]^+$ Calcd for $C_{26}H_{24}BF_2N_3O$ 444.2058; Found 444.2052.

■ ASSOCIATED CONTENT

Supporting Information

Absorption and emission spectra for benchmark monomers, fluorescence data for selected dyads in different solvents, and copies of ^{1}H, ^{13}C, and ^{19}F NMR spectra for new compounds. This material is available free of charge via the Internet at http://pubs.acs.org.

■ AUTHOR INFORMATION

Corresponding Author

*E-mail: mptaszek@umbc.edu (M.P.).

Author Contributions

†These authors contributed equally to this work.

Notes

The authors declare no competing financial interest.

■ ACKNOWLEDGMENTS

This work was supported by the University of Maryland, Baltimore County (start-up funds and SRAIS Award), and by the National Cancer Institute of the National Institutes of Health under Award Number U01CA181628. The content is solely the responsibility of the authors and does not necessarily represent the official views of the National Institutes of Health. We thank Ms. Lauren N. Resch for a thorough proofreading of the manuscript.

■ REFERENCES

(1) Tamiaki, H.; Kunieda, M. In *Handbook of Porphyrin Sciences*; Kadish, K. M., Smith, K. M., Guilard, R., Eds.; World Scientific Publishing: Hackensack, NJ, 2011; Vol. *11*, pp 223−285.

(2) Yang, E.; Kirmaier, C.; Krayer, M.; Taniguchi, M.; Kim, H.-J.; Diers, J. R.; Bocian, D. F.; Lindsey, J. S.; Holten, D. *J. Phys. Chem. B* **2011**, *115*, 10801−10816.

(3) Kee, H. L.; Kirmaier, C.; Tang, Q.; Diers, J. R.; Muthiah, C.; Taniguchi, M.; Laha, J. K.; Ptaszek, M.; Lindsey, J. S.; Bocian, D. F.; Holten, D. *Photochem. Photobiol.* **2007**, *83*, 1110−1124.

(4) Kee, H. L.; Kirmaier, C.; Tang, Q.; Diers, J. R.; Muthiah, C.; Taniguchi, M.; Laha, J. K.; Ptaszek, M.; Lindsey, J. S.; Bocian, D. F.; Holten, D. *Photochem. Photobiol.* **2007**, *83*, 1125−1143.

(5) Taniguchi, M.; Cramer, D. L.; Bhise, A. D.; Kee, H. L.; Bocian, D. F.; Holten, D.; Lindsey, J. S. *New J. Chem.* **2008**, *32*, 947−958.

(6) Vinita, A. M.; Sano, K.; Yu, Z.; Nakajima, T.; Choyke, P.; Ptaszek, M.; Kobayashi, H. *Bioconjugate Chem.* **2012**, *23*, 1671−1679.

(7) Harada, T.; Sano, K.; Sato, K.; Watanabe, R.; Yu, Z.; Hanaoka, H.; Nakajima, T.; Choyke, P. L.; Ptaszek, M.; Kobayashi, H. *Bioconjugate Chem.* **2014**, *25*, 362−369.

(8) (a) Resch-Genger, U.; Grabolle, M.; Cavaliere-Jaricot, S.; Nitschke, R.; Nann, T. *Nat. Methods* **2008**, *5*, 763−775. (b) Raines, R. T.; Lavis, L. D. *ACS Chem. Biol.* **2008**, *3*, 142−155.

(9) Lovell, J. F.; Chan, M. W.; Qi, Q.; Chen, J.; Zheng, G. *J. Am. Chem. Soc.* **2011**, *133*, 18580−18582.

(10) (a) Cao, W.; Ng, K. K.; Corbin, I.; Zhang, Z.; Ding, L.; Chen, J.; Zheng, G. *Bioconjugate Chem.* **2009**, *20*, 2023−2031. (b) Liu, T. W.; Akens, M. K.; Chen, J.; Wise-Milestone, L.; Wilson, B. C.; Zheng, G. *Bioconjugate Chem.* **2011**, *22*, 1021−1030. (c) Mawn, T. M.; Popov, A. V.; Beardsley, N. J.; Stefflova, K.; Milkevitch, M.; Zheng, G.; Delikatny, E. J. *Bioconjugate Chem.* **2011**, *22*, 2434−2443. (d) Popov, A. V.; Mawn, T. M.; Kim, S.; Zheng, G.; Delikatny, E. J. *Bioconjugate Chem.* **2010**, *21*, 1724−1727. (e) Liu, T. W. B.; Chen, J.; Burgess, L.; Cao, W.; Shi, J.; Wilson, B. C.; Zheng, G. *Theranostics* **2011**, *1*, 354−362. (f) Lovell, J. F.; Jin, C. S.; Huynh, E.; Jin, H.; Kim, C.; Rubinstein, J. L.; Chan, W. C. W.; Cao, W.; Wang, L. V.; Zheng, G. *Nat. Mater.* **2011**, *10*, 324−332. (g) Huynh, E.; Jin, C. S.; Wilson, B. C.; Zheng, G. *Bioconjugate Chem.* **2014**, *25*, 796−801.

(11) Strachan, J.-P.; O'Shea, D. F.; Balasubramanian, T.; Lindsey, J. S. *J. Org. Chem.* **2000**, *65*, 3160−3172.

(12) Kim, H.-J.; Lindsey, J. S. *J. Org. Chem.* **2005**, *70*, 5475−5486.

(13) Umezawa, K.; Matsui, A.; Nakamura, Y.; Citterio, D.; Suzuki, K. *Chem.—Eur. J.* **2009**, *15*, 1096−1106.

(14) Taniguchi, M.; Ra, D.; Kirmaier, C.; Hindin, E.; Schwartz, J. K.; Diers, J. R.; Knox, R. S.; Bocian, D. F.; Lindsey, J. S.; Holten, D. *J. Am. Chem. Soc.* **2003**, *125*, 13461−13470.

(15) Muthukumaran, K.; Loewe, R. S.; Kirmaier, C.; Hindin, E.; Schwartz, J. K.; Sazanovich, I. V.; Diers, J. R.; Bocian, D. F.; Holten, D.; Lindsey, J. S. *J. Phys. Chem. B* **2003**, *107*, 3431−3422.

(16) Muthiah, C.; Kee, H. L.; Diers, J. R.; Fan, D.; Ptaszek, M.; Bocian, D. F.; Holten, D.; Lindsey, J. S. *Photochem. Photobiol.* **2008**, *84*, 786−801.

(17) Kee, H. L.; Nothdurft, R.; Muthiah, C.; Diers, J. R.; Fan, D.; Ptaszek, M.; Bocian, D. F.; Lindsey, J. S.; Culver, J. P.; Holten, D. *Photochem. Photobiol.* **2008**, *84*, 1061−1072.

(18) Kee, H. L.; Diers, R. J.; Ptaszek, M.; Muthiah, C.; Fan, D.; Bocian, D. F.; Lindsey, J. S.; Culver, J. P.; Holten, D. *Photochem. Photobiol.* **2009**, *85*, 909−920.

(19) Laakso, J.; Rosser, G. A.; Szijjártó, C.; Beeby, A.; Borbas, K. E. *Inorg. Chem.* **2012**, *51*, 10366−10374.

(20) Yu, Z.; Ptaszek, M. *J. Org. Chem.* **2013**, *78*, 10678−10691.

(21) Voznyak, D. A.; Zakharova, G. V.; Chibisov, A. K.; Kharitonova, O. V.; Grin, M. A.; Semenikhin, K. O.; Mironov, A. F. *High Energy Chem.* **2010**, *44*, 31−36.

(22) Kataoka, Y.; Shibata, Y.; Tamiaki, H. *Chem. Lett.* **2010**, *39*, 953−955.

(23) Finikova, O. S.; Troxler, T.; Senes, A.; DeGrado, W. F.; Hochstrasser, R. M.; Vinogradov, S. A. *J. Phys. Chem. A* **2007**, *111*, 6977−6990.

(24) Mani, T.; Niedzwiedzki, D. M.; Vinogradov, S. A. *J. Phys. Chem. A* **2012**, *116*, 3568−3610.

(25) (a) Loudet, A.; Burgess, K. *Chem. Rev.* **2007**, *107*, 4891−4932. (b) Ziessel, R.; Ulrich, G.; Harriman, A. *New J. Chem.* **2007**, *31*, 496−501. (c) Boens, N.; Leen, V.; Dehaen, W. *Chem. Soc. Rev.* **2012**, *41*, 1130−1172. (d) Ziessel, R.; Harriman, A. *Chem. Commun.* **2011**, *47*, 611−631. (e) El-Khouly, M. E.; Fukuzumi, S.; D'Souza, F. *ChemPhysChem* **2014**, *15*, 30−47.

(26) Some recent representative examples: (a) Erbas-Cakmak, S.; Akkaya, E. U. *Org. Lett.* **2014**, *16*, 2964−2949. (b) Kostereli, T.; Ozdemir, T.; Buyukcakir, O.; Akkaya, E. U. *Org. Lett.* **2012**, *14*, 3636−3639. (c) Ziessel, R.; Ulrich, G.; Haefele, A.; Harriman, A. *J. Am. Chem. Soc.* **2013**, *135*, 11330−11344. (d) Harriman, A.; Mallon, L. J.; Elliot, K. J.; Haefele, A.; Ulrich, G.; Ziessel, R. *J. Am. Chem. Soc.* **2009**, *131*, 13375−13386. (e) Thivierge, C.; Han, J.; Jenkins, R. M.; Burgess, K. *J. Org. Chem.* **2011**, *76*, 4219−5228. (f) Wu, L.; Loudet, A.; Barhoumi, R.; Burghardt, R. C.; Burgess, K. *J. Am. Chem. Soc.* **2009**, *131*, 9156−9157. (g) Zhang, X.; Xiao, Y.; He, L.; Zhang, Y. *J. Org. Chem.* **2014**, *79*, 6315−6320. (h) Pochorovski, I.; Knehans, T.; Nettels, D.; Müller, A. M.; Schweizer, B.; Caflisch, A.; Schuler, B.; Diederich, F. *J. Am. Chem. Soc.* **2014**, *136*, 2441−2449. (i) Zhang, C.; Zhao, J.; Wu, S.; Wang, Z.; Wu, W.; Ma, J.; Gao, S.; Huang, L. *J. Am. Chem. Soc.* **2013**, *135*, 10566−10578.

(27) (a) Ueno, Y.; Jose, J.; Loudet, A.; Pérez-Bolivar, C.; Anzenbacher, P., Jr.; Burgess, K. *J. Am. Chem. Soc.* **2011**, *133*, 51−55. (b) Shi, W.-J.; El-Khouly, M. E.; Ohkubo, K.; Fukuzumi, S.; Ng, D. K. P. *Chem.—Eur. J.* **2013**, *19*, 11332−11341. (c) Bandi, V.; Ohkubo, K.; Fukuzumi, S.; D'Souza, F. *Chem. Commun.* **2013**, *49*, 2867−2869. (d) Bandi, V.; El-Khouly, M. E.; Nesterov, V. N.; Karr, P. A.; Fukuzumi, S.; D'Souza, F. *J. Phys. Chem. C* **2013**, *117*, 5638−5649. (e) El-Khouly, M. E.; Amin, A. N.; Zandler, M. E.; Fukuzumi, S.; D'Souza, F. *Chem.—Eur. J.* **2013**, *18*, 4239−5247. (f) Liu, J.-Y.; Ermilov, E. A.; Röder, B.; Ng, D. K. P. *Chem. Commun.* **2009**, 1517−

DOI: 10.1021/acs.joc.5b00119
J. Org. Chem. 2015, 80, 3858−3869

1519. (g) Liu, J.-Y.; Huang, Y.; Menting, R.; Röder, B.; Ermilov, B.; Ng, D. K. P. *Chem. Commun.* **2013**, *49*, 2998−3000.
(28) Khan, T. K.; Bröring, M.; Mathur, S.; Ravikanth, M. *Coord. Chem. Rev.* **2013**, *257*, 2348−2387.
(29) Rio, Y.; Seitz, W.; Gouloumis, A.; Vázquez, P.; Sessler, J. L.; Guldi, D. M.; Torres, T. *Chem.—Eur. J.* **2010**, *16*, 1929−1940.
(30) (a) Kirmaier, C.; Hindin, E.; Schwartz, J. K.; Sazanovich, I. V.; Diers, J. R.; Muthukumaran, K.; Taniguchi, M.; Bocian, D. F.; Lindsey, J. S.; Holten, D. *J. Phys. Chem. B* **2003**, *107*, 3443−3454. (b) Kelley, R. F.; Tauber, M. J.; Wasielewski, M. R. *J. Am. Chem. Soc.* **2006**, *128*, 4779−4791. (c) Gunderson, V. L.; Smeigh, A. L.; Kim, C. H.; Co, D. T.; Wasielewski, M. R. *J. Am. Chem. Soc.* **2012**, *134*, 4363−4372.
(31) Sunahara, H.; Urano, Y.; Kojima, H.; Nagano, T. *J. Am. Chem. Soc.* **2007**, *129*, 5597−5604.
(32) Ptaszek, M.; Lahaye, D.; Krayer, M.; Muthiah, C.; Lindsey, J. S. *J. Org. Chem.* **2010**, *75*, 1659−1673.
(33) Laha, J. K.; Muthiah, C.; Taniguchi, M.; McDowell, B.; Ptaszek, M.; Lindsey, J. S. *J. Org. Chem.* **2006**, *71*, 4092−4102.
(34) (a) Ast, S.; Fischer; Müller, H.; Mickler, W.; Schwichtenberg, M.; Rurack, K.; Holdt, H.-J. *Chem.—Eur. J.* **2013**, *19*, 2990−3005. (b) Bura, T.; Nastasi, F.; Puntoriero, F.; Campagna, S.; Ziessel, R. *Chem.—Eur. J.* **2013**, *19*, 8900−8912. (c) Godoy, J.; Vives, G.; Tour, J. M. *Org. Lett.* **2010**, *12*, 1464−1467. (d) Hayek, A.; Bolze, F.; Bourgogne, C.; Baldeck, P. L.; Didier, P.; Arntz, Y.; Mély, Y.; Nicoud, J.-F. *Inorg. Chem.* **2009**, *48*, 9112−9119.
(35) Yu, Z.; Ptaszek, M. *Org. Lett.* **2012**, *14*, 3708−3711.
(36) Chen, Y.; Wang, H.; Wan, L.; Bian, Y.; Jiang, J. *J. Org. Chem.* **2011**, *76*, 3774−3781.
(37) Ambroise, A.; Li, J.; Yu, L.; Lindsey, J. S. *Org. Lett.* **2000**, *2*, 2563−2566.
(38) Wu, L.; Loudet, A.; Barhoumi, R.; Burghardt, R. C.; Burgess, K. *J. Am. Chem. Soc.* **2009**, *131*, 9156−9157.
(39) (a) Fortage, J.; Göransson, E.; Blart, E.; Becker, H.-C.; Hammarström, L.; Odobel, F. *Chem. Commun.* **2007**, 4629−4631. (b) Fortage, J.; Boixel, J.; Blart, E.; Hammarström, L.; Becker, H. C.; Odobel, F. *Chem.—Eur. J.* **2008**, *14*, 3467−3480. (c) Wielopolski, M.; Atienza, C.; Clark, T.; Guldi, D. M.; Martin, N. *Chem.—Eur. J.* **2008**, *14*, 6379−6390.
(40) Ptaszek, M.; Bhaumik, J.; Kim, H.-J.; Taniguchi, M.; Lindsey, J. S. *Org. Process Res. Dev.* **2005**, *9*, 651−659.
(41) Krayer, M.; Balasubramanian, T.; Ruzié, C.; Ptaszek, M.; Cramer, D. L.; Taniguchi, M.; Lindsey, J. S. *J. Porphyrins Phthalocyanines* **2009**, *13*, 1098−1110.

DOI: 10.1021/acs.joc.5b00119
J. Org. Chem. 2015, 80, 3858−3869